Biochimica et Biophysica Acta 1843 (2014) 2356–2364

Contents lists available at ScienceDirect

Biochimica et Biophysica Acta

journal homepage: www.elsevier.com/locate/bbamcr

Quantitative evaluation of the cell penetrating properties of an iodinated Tyr-L-maurocalcine analog ☆

Céline Tisseyre [a,b], Mitra Ahmadi [b,c], Sandrine Bacot [b,c], Lucie Dardevet [a,b], Pascale Perret [b,c], Michel Ronjat [a,b], Daniel Fagret [b,c], Yves Usson [b,e], Catherine Ghezzi [b,c], Michel De Waard [a,b,d,*]

[a] INSERM, U836, Grenoble Institute of Neuroscience, LabEx Ion Channels, Science and Therapeutics, Grenoble, France
[b] Université Joseph Fourier, Grenoble, France
[c] INSERM, U1039, Radiopharmaceutiques Biocliniques, Grenoble, France
[d] Smartox Biotechnologies, Grenoble, France
[e] CNRS, UMR5525, TIMC-IMAG, Grenoble, France

ARTICLE INFO

Article history:
Received 3 January 2014
Received in revised form 27 February 2014
Accepted 17 March 2014
Available online 22 March 2014

Keywords:
Maurocalcine
Cell penetrating peptide
Radioiodination
Quantitative evaluation
Drug delivery

ABSTRACT

L-Maurocalcine (L-MCa) is the first reported animal cell-penetrating toxin. Characterizing its cell penetration properties is crucial considering its potential as a vector for the intracellular delivery of drugs. Radiolabeling is a sensitive and quantitative method to follow the cell accumulation of a molecule of interest. An L-MCa analog containing an additional N-terminal tyrosine residue (Tyr-L-MCa) was synthesized, shown to fold and oxidize properly, and successfully radioiodinated to ^{125}I-Tyr-L-MCa. Using various microscopy techniques, the average volume of the rat line F98 glioma cells was evaluated at 8.9 to 18.9 × 10^{-7} μl. ^{125}I-Tyr-L-MCa accumulates within cells with a dose-dependency similar to the one previously published using 5,6-carboxyfluorescein-L-MCa. According to subcellular fractionation of F98 cells, plasma membranes keep less than 3% of the peptide, regardless of the extracellular concentration, while the nucleus accumulates over 75% and the cytosol around 20% of the radioactive material. Taking into account both nuclear and cytosolic fractions, cells accumulate intracellular concentrations of the peptide that are equal to the extracellular concentrations. Estimation of ^{125}I-Tyr-L-MCa cell entry kinetics indicate a first rapid phase with a 5 min time constant for the plasma membrane followed by slower processes for the cytoplasm and the nucleus. Once inside cells, the labeled material no longer escapes from the intracellular environment since 90% of the radioactivity remains 24 h after washout. Dead cells were found to have a lower uptake than live ones. The quantitative information gained herein will be useful for better framing the use of L-MCa in biotechnological applications. This article is part of a Special Issue entitled: Calcium Signaling in Health and Disease. Guest Editors: Geert Bultynck, Jacques Haiech, Claus W. Heizmann, Joachim Krebs, and Marc Moreau.

1. Introduction

Crossing cellular membranes represents a major hurdle in current drug development. Cell-penetrating peptides (CPP) are molecular vectors that enter cells and allow the intracellular delivery of a number of bioactive molecules such as drugs, peptides, proteins, oligonucleotides/cDNA/RNA, and nanoparticles [1–3]. Originally isolated from the venom of the scorpion *Scorpio maurus palmatus* [4], L-maurocalcine (L-MCa) is a highly basic, positively charged, 33-mer peptide that efficiently binds to the ryanodine receptor in skeletal muscles and promotes channel opening and calcium release from the sarcoplasmic reticulum. The binding site of L-MCa on the ryanodine receptor has been identified as cytoplasmic [5], suggesting that cytoplasmic application is required for its pharmacological effect. The fast kinetics (few seconds) at which extracellular application of L-MCa triggers internal Ca^{2+} release indicates that the peptide should be able to easily translocate through the plasma membrane [6]. According to ^{1}H NMR analysis, the peptide presents three disulfide bridges (Cys^{3}–Cys^{17}, Cys^{10}–Cys^{21} and Cys^{16}–Cys^{32}) and folds along an inhibitor cysteine knot pattern [4,7]. It contains three β-strands from amino acid residues 9–11 (strand 1), 20–23 (strand 2), and 30–33 (strand 3) with strands 2 and 3 forming an antiparallel β-sheet (Fig. 1A). Several lines of experimental evidence indicate that L-MCa is a member of the exponentially growing family of CPPs [6,8–13]. The peptide is highly efficient in entering a variety of cell types compared to other popular CPP such as TAT or penetratin. It presents a low toxicity profile (absence of toxicity at concentrations above 10 μM) [8], penetrates at lower concentrations [14], and efficiently accumulates into the cytoplasm which is a highly desirable feature for many biotechnological applications that require the use of CPP. Therefore, a quantitative

☆ This article is part of a Special Issue entitled: Calcium Signaling in Health and Disease. Guest Editors: Geert Bultynck, Jacques Haiech, Claus W. Heizmann, Joachim Krebs, and Marc Moreau.

* Corresponding author at: INSERM, U836, Grenoble Neuroscience Institute, Site Santé de la Tronche, Bâtiment Edmond J. Safra, 38042 Grenoble Cedex 09, France. Tel.: +33 456 520 563; fax: +33 456 520 637.
E-mail address: michel.dewaard@ujf-grenoble.fr (M. De Waard).

http://dx.doi.org/10.1016/j.bbamcr.2014.03.017
0167-4889/

assessment of the cell penetration properties of L-MCa is of great importance considering its potential as a vector for the improved delivery of therapeutic compounds. Radiolabeling represents the most sensitive and quantitative method to follow the quantitative entry of a cell penetrating peptide of interest. Radioiodination is a widely used method for radiolabeling of chemical compounds since the presence of iodine would poorly affects the structural properties of the molecule of interest. Specifically, ^{125}I radiolabeling is commonly performed for *in vitro* radioligand interaction and *in vivo* biodistribution studies [15,16]. For the purpose of radiolabeling of L-MCa, we synthesized an analog with an extra amino-terminal tyrosine residue, termed Tyr-L-MCa, that still possesses the pharmacological properties of wild-type L-MCa. Next, we quantitatively investigated the cell penetration properties of the radioiodinated Tyr-L-MCa using the rat F98 glioma cell line and a precise evaluation of cell volume by Digital Holographic Microscopy (DHM) or by confocal microscopy (CM). The results of the present study will be useful for future *in vivo* biodistribution studies of MCa.

2. Material and methods

2.1. Materials

N-α-Fmoc-L-amino acid, Wang-Tentagel resin and reagents used for peptide synthesis were obtained from Iris Biotech. Solvents were analytical grade products from Acros Organics. Acetonitrile was High Performance Liquid Chromatography (HPLC) gradient grade from Fischer Scientific and trifluoroacetic acid (purum ≥98%) from Fluka

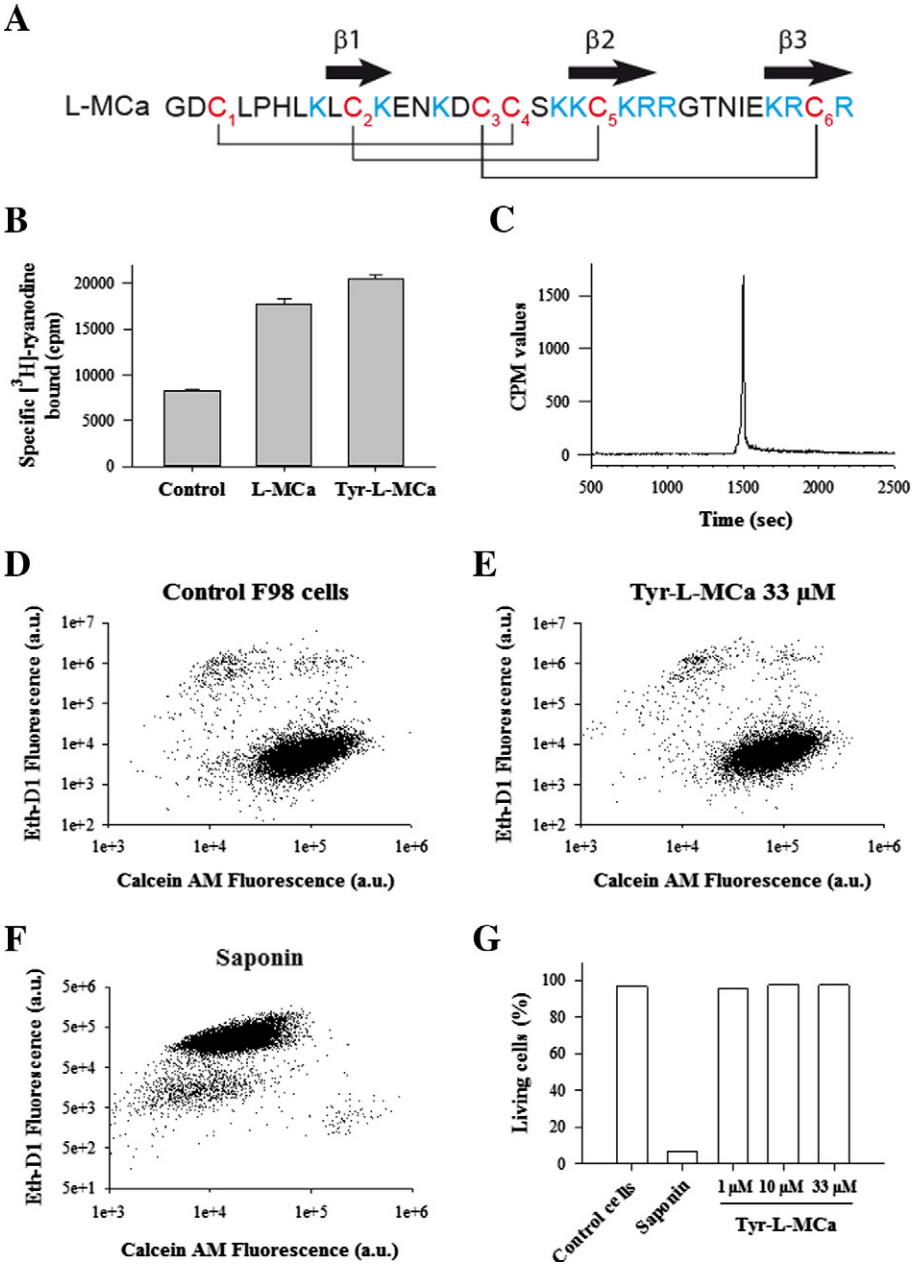

Fig. 1. Properties of the Tyr-L-MCa analog. (A) Primary structure of L-MCa. The disulfide bridge connectivity is shown by lines connecting the six semi-cystine residues. The positions of the three β-strands are indicated by arrows. Blue residues denote basic amino acids. (B) Stimulation of [^{3}H]-ryanodine binding onto SR vesicles. Experimentally, binding was performed at pCa = 5 which explains why L-MCa stimulation of binding is limited. No significant differences were observed between the efficacies of L-MCa and Tyr-L-MCa. (C) RP-HPLC profile of ^{125}I-Tyr-L-MCa after radiolabeling. Note the homogeneous labeling of the peptide by ^{125}I. (D) Cell viability assay by flow cytometry for control F98 cells. The ethidium-D1 fluorescence level measures cell death level. (E) Cell viability assay by flow cytometry for F98 cells after 2 h incubation with 33 µM Tyr-L-MCa. (F) Cell viability assay by flow cytometry for F98 cells after 5 min incubation with 0.1% saponin. Note the extensive cell death produced by saponin. (G) Proportion of live F98 cells for control, saponin and Tyr-L-MCa conditions.

and lactoperoxidase of bovine milk (80 IU/mg) were from Sigma-Aldrich, hydrogen peroxide 30% in water (w/w) from Carlo Erba and $Na^{125}I$ (3.7 GBq/ml) from Perkin Elmer. DMEM F-12 medium with or without phenol red, fetal bovine serum, Trypsin-EDTA, rhodamine-conjugated concanavalin A and live/dead viability/cytotoxicity kit were obtained from Invitrogen. Protease inhibitors (cOmplete Min, EDTA-free) were from Roche diagnostics.

2.2. Synthesis of Tyr-L-MCa by solid-phase

Tyr-L-MCa with an extra N-terminal tyrosyl residue was synthetized to allow L-MCa radioiodination. Chemical synthesis of Tyr-L-MCa was performed as previously described [17] with the following modifications. Briefly, Tyr-L-MCa was chemically synthesized by the solid-phase peptide synthesis (SPPS) method [18] using an automated peptide synthesizer (CEM© Liberty). The peptide chain was assembled stepwise on 0.24 mEq of Fmoc-L-Arg(Pbf)-Wang-Tentagel resin using 0.24 mmol of N-α-fluorenylmethyloxycarbonyl (Fmoc) L-amino-acid derivatives. The side-chain protecting groups were Trityl for Cys and Asn, *tert*-butyl for Ser and Tyr, Thr, Glu and Asp, Pbf for Arg, and *tert*-butylcarbonyl for Lys. Reagents were at the following concentrations: 0.2 M Fmoc-amino-acids (Fmoc-AA-OH in dimethylformamide (DMF)), 0.5 M activator (2-(1H-benzotriazole-1-yl)-1,1,3,3-tetramethyluronium hexafluorophosphate in DMF), 2 M activator base (diisopropylethylamine in N-methyl-pyrrolidone) and deprotecting agent (5% piperazine/0.1 M 1-hydroxybenzotriazole in DMF), as advised by PepDriver (CEM©). After peptide chain assembly, the resin was treated with a mixture of trifluoroacetic acid/water/triisopropylsilane/1,4-dithiothreitol (92.5/2.5/2.5/2.5) for 4 h at room temperature. The peptide mixture was then filtered to eliminate the resin and the filtrate was precipitated by adding cold *t*-butylmethyl ether. The crude peptide was pelleted by centrifugation (10,000 ×*g*, 15 min) and the supernatant was discarded. The crude and reduced Tyr-L-MCa was submitted to oxidation for disulfide bridge formation in 0.1 M Tris/HCl buffer at pH 8.2 during 3 days at room temperature. Oxidized/folded Tyr-L-MCa was then purified by HPLC using a Vydac C18 column (218TP1010, 250 × 10 mm). Elution of the peptide was performed with a 10–60% acetonitrile linear gradient containing 0.1% trifluoroacetic acid (TFA) over 40 min. The purity of the collected fraction was analyzed by reversed phase (RP)-HPLC using analytical C18 column (Vydac, 218TP104, 10 μm, 250 × 4.6 mm). Tyr-L-MCa was characterized by MALDI-TOF mass spectrometry. Samples were mixed 1:1 (v/v) with 10 mg/ml α-cyano-4-hydroxycinnamic acid (HCCA) before spotted onto a MALDI target plate. Mass spectrometry analyses were performed on a 4800 MALDI-TOF/TOF instrument (ABSciex). MS spectra were acquired in positive ion reflector mode over a mass range of 800–6000 m/z.

2.3. Radiolabeling of Tyr-L-MCa using lactoperoxidase

^{125}I-Tyr-L-MCa was prepared using a direct iodination procedure with lactoperoxidase/H_2O_2 system as oxidant. Briefly, 37 MBq of ^{125}I were added to 10 μg of Tyr-MCa in phosphate buffer (50 mM, pH 7.4). The reaction was allowed to proceed for 30 min at room temperature after addition of lactoperoxidase and H_2O_2 at a final concentration of 0.5 μM and 25 μM respectively. Radioiodinated Tyr-L-MCa was analyzed by HPLC immediately and radiochemical purity higher than 95% was achieved, thereby obviating the need for a purification step. A single peak of radioiodinated ^{125}I-Tyr-L-MCa was observed. The compound was stable for over 48 h. A similar labeling was performed with $Na^{127}I$ according to the same procedure. In these conditions, the compound was shown to be monoiodinated (not shown). The resulting compounds, ^{125}I-Tyr-L-MCa and ^{127}I-Tyr-L-MCa, were mixed in order to obtain a specific activity of 0.4 MBq/nmol of Tyr-L-MCa (activimeter Capintec). Hereafter, we shall speak about ^{125}I-Tyr-L-MCa although it reflects a mixture of ^{125}I-Tyr-L-MCa and ^{127}I-Tyr-L-MCa.

2.4. F98 glioma cell culture

All experiments were performed using the F98 glioblastoma cancer cell line (undifferentiated malignant glioma rat cell line from ATCC) maintained at 37 °C in 5% CO_2 in DMEM F-12 medium supplemented with 2% (v/v) heat-inactivated fetal bovine serum and 10,000 units/ml streptomycin and penicillin. Cells were platted on 24 well plates (Falcon; 700,000 cells/well) and grown 24 h until they reach 90% confluence.

2.5. Cell counting

To get a precise estimate of the cell number present in each well at the time where cell penetration experiments are performed with ^{125}I-Tyr-L-MCa, F98 cells were counted by flow cytometry analyses with live cells using a Becton Dickinson Accuri C6 flow cytometer (BD Biosciences). Data were obtained and analyzed using BD Accuri C6 software. Live cells were gated by forward/side scattering.

2.6. Evaluation of F98 cell death

Cells were incubated with or without various concentrations of Tyr-L-MCa during 2 h. Cells were washed with PBS and washes were conserved. They were then treated with 0.05% trypsin-EDTA for 5 min at 37 °C to detach them from the support. Cells were collected and resuspended in DMEM-F12 with 2% fetal bovine serum along with the initial washes. For one series of control cells, 0.1% saponin was added just before centrifugation to induce cell death. All cell conditions (control, Tyr-L-MCa and saponin) were centrifuged at 800 ×*g* during 5 min. The pellets were resuspended in 200 μl of staining mix according to Invitrogen recommendations. Cells were left in the dark for 15 min at room temperature before analyses by flow cytometry using the LIVE/DEAD® Viability/Cytotoxicity Kit of Invitrogen. This kit quickly discriminates live from dead cells by simultaneously staining with green-fluorescent calcein-AM to indicate intracellular esterase activity and red-fluorescent ethidium homodimer-1 to indicate loss of plasma membrane integrity. Similar results were obtained with ^{125}I-Tyr-L-MCa.

2.7. Estimation of F98 cell volume by Digital Holographic Microscopy or confocal microscopy

Digital Holographic Microscopy (DHM) is an interferometric technique that makes possible the imaging and measurement of the phase retardation through transparent biological specimen [19]. Because it is based on the interference of coherent light (lambda 658 nm) a high precision (nm order) can be obtained in optical thickness measurements. Under the hypothesis of invariance of the refractive index within the cytosol, it may be admitted that the measured optical thickness is a good estimate of the quantity of matter traversed by light [20]. Therefore, the average F98 cell volume was estimated by integrating the optical thickness over the projected area of each cell.

To evaluate the F98 cell volume by confocal microscopy, cell plasma membranes were stained with 50 μg/ml concanavalin A-rhodamine for 5 min. Next, cells were washed with phosphate buffered saline (PBS) and incubated in DMEM without phenol red. Live cells were then immediately analyzed by confocal laser scanning microscopy using a Zeiss LSM operating system. Rhodamine was sequentially excited (at 561 nm) and emission fluorescence (at 590 nm) was collected. Stacks of 17 to 22 confocal images were taken by steps of 1 μm on the z-axis to cover the entire depth of the cells. Globally, F98 cells were quite thick but some images of the stacks may not contain any information. Next, a dedicated Image J macro was developed to reconstruct the 3-D

F98 cell image to calculate the global volume using the stained plasma membrane boundaries.

2.8. Quantitative evaluation of the cell penetration of ^{125}I-Tyr-L-MCa

F98 cells were incubated with various concentrations of radioiodinated ^{125}I-Tyr-L-MCa (33 nM to 10 μM) in DMEM F-12 culture medium (200 to 400 μl per well) without serum or antibiotics at 37 °C for 2 h to allow cell penetration. For the estimation of the kinetics of cell entry of the compound, the time of incubation could be shortened as indicated. Each concentration contained 2.5% of ^{125}I-radiolabeled peptide and 97.5% of ^{127}I-labeled peptide to diminish the quantity of radioactive peptide to handle. After incubation, the cells were washed twice with PBS to remove excess extracellular peptide. They were then treated with 0.05% trypsin-EDTA for 5 min at 37 °C to (i) degrade any remaining extracellular ^{125}I-Tyr-L-MCa and (ii) detach F98 cells from the surface. Cells were collected and resuspended in DMEM-F12 with 2% fetal bovine serum. Cells were centrifuged at 800 ×*g* during 5 min. The pellet was resuspended in PBS and cells were then centrifuged a second time in the same conditions. Of note, for each one of the centrifugation and washing steps, resuspended cells were transferred to new tubes to eliminate any extracellular radioiodinated ^{125}I-Tyr-L-MCa or trypsin-induced fragment that may be potentially present by sticking to the plastic. Cells were resuspended in 1 ml of lysis buffer (in mM: Tris 20, NaCl 150, DTT 1, sucrose 250, pH 8.0 along with protease inhibitors) and incubated on ice for 5 min. Next, cells were mechanically disrupted using a potter. Subcellular fractionation was performed as follows. First, the cell lysates were centrifuged at 900 ×*g* for 20 min and the pellet containing the cell nuclei (F98-N) was collected. Next, the supernatant was collected and centrifuged at 50.000 ×*g* for 60 min. The pellet containing the plasma membrane was kept (F98-PM) along with the supernatant that represents the cytoplasm (F98-C). Both pellets were resuspended in 500 μl distilled water for counting. This subcellular fractionation method separates membrane-bound (F98-PM) from intracellular ^{125}I-Tyr-L-MCa (F98-N + F98-C) providing an estimate of cell penetration of the peptide into the cytoplasm. Counting of radioactivity was carried out by gamma-well counter.

2.9. Determination of the intracellular concentration of ^{125}I-Tyr-L-MCa

Knowing the precise cell number per well, the average cell volume and the specific activity of ^{125}I-Tyr-L-MCa, we were able to convert counts per min to intracellular peptide concentration. The concentration of radioiodinated Tyr-L-MCa is provided in μM and was calculated according to the equation $f_0 = (((cpm/cell\ number)/a)/b)/cell\ volume$. The value **a** is a constant value of the gamma-well counter (a = 35515679 to convert cpm values in MBq). The value **b** is the specific activity of Tyr-L-MCa that has been used for the preparation of dilutions. Only the added values of F98-N and F98-C radioactivity were taken into account to quantify cell penetration. F98-PM values were discarded.

2.10. Kinetic of cellular leakage of ^{125}I-Tyr-L-MCa

F98 cells were incubated with 1 μM of ^{125}I-Tyr-L-MCa in DMEM F-12 culture medium without serum or antibiotics at 37 °C for 2 h. The cells were then washed three times with PBS to remove excess extracellular peptide, and then completed with DMEM F-12 medium. At different times (0, 1, 2, 3, 4, 5, 6 and 24 h), a sample of 100 μl of medium was taken for radioactivity counting and replaced by 100 μl of fresh complete medium. The value obtained was corrected by a factor of 4 (100 μl taken out of 400 μl of medium). A control was performed without cells to demonstrate that the plastic of the wells did not release any radioactivity. The quantity of radioactivity released by the cells was evaluated as a ratio of total cell radioactivity as determined previously.

2.11. [^{3}H]-ryanodine binding on ryanodine receptors from skeletal muscle heavy SR vesicles

Heavy sarcoplasmic reticulum (SR) vesicles were prepared as described [11]. Protein concentration was measured by the Biuret method. Heavy SR vesicles (1 mg/ml) were incubated at 37 °C for 2 h in an assay buffer composed of 10 nM [^{3}H]-ryanodine, 150 mM KCl, 2 mM EGTA, 2 mM $CaCl_2$ (pCa = 5), and 20 mM MOPS, pH 7.4. 200 nM L-MCa or Tyr-L-MCa was added prior to the addition of heavy SR vesicles. [^{3}H]-ryanodine bound to heavy SR vesicles was measured by filtration through Whatman GF/B glass filters followed by three washes with 5 ml of ice-cold washing buffer composed of 150 mM NaCl, 20 mM HEPES, pH 7.4. [^{3}H]-ryanodine retained on the filters was measured by liquid scintillation. Nonspecific binding was measured in the presence of 80 μM unlabeled ryanodine. The data are presented as mean ± S.E. Each experiment was performed in triplicate.

3. Results

3.1. Tyr-L-MCa: a functional MCa analog for iodination

L-MCa itself lacks a tyrosine residue for radio-iodination of the peptide. To this end, we produced a new analog of L-MCa with an extra amino-terminal tyrosine residue. Earlier observations had demonstrated that N-terminal-modified analogs of L-MCa could be easily produced since the addition of an extra-biotinylated lysine residue is without impact on the proper folding/oxidation of the peptide [9]. MS analyses (MALDI-TOF technique) of crude and folded/oxidized Tyr-L-MCa provide experimental molecular masses $(M + H)^+$ of 4026.9 and 4020.8 Da, respectively. The shift in experimental molecular mass of 6.1 Da upon folding/oxidation is in agreement with the engagement of all six cysteine residues in the formation of three disulfide bridges. Since the activity of L-MCa is strictly dependent on the proper/folding of the peptide [21] and that this activity is not altered by N-terminal modification [6,9], it is expected that Tyr-L-MCa should have preserved its pharmacological effect. Fig. 1B illustrates that this is indeed the case. As shown, Tyr-L-MCa turned as potent as L-MCa itself in stimulating the binding of [^{3}H]-ryanodine onto skeletal muscle ryanodine receptors from SR vesicles. Next, since Tyr-L-MCa remained functional, the peptide was enzymatically iodinated using the lactoperoxidase/H_2O_2 system. Under the experimental conditions described radiochemical purity higher than 95% was achieved. This was further illustrated in the HPLC profile of the compound (Fig. 1C). ^{125}I-Tyr-L-MCa remained stable for over 24 h. ^{127}I iodination was also used to prepare ^{127}I-Tyr-L-MCa instead of ^{125}I-Tyr-L-MCa to lower the specific activity and the quantity of radioactivity to handle. Modeling experiments illustrates the relative position of the extra iodinated tyrosine residue onto L-MCa (Fig. 2).

3.2. Tyr-L-MCa lacks cell toxicity and is partially degraded by trypsin treatment

We first assessed that Tyr-L-MCa does not induce cell death that may alter the evaluation of cell penetration. For that purpose, we used rat glioma F98 cells because we plan to use L-MCa as a vector for the delivery of chemo-active drugs in later studies. As shown by flow cytometry, incubating F98 cells 2 h with 33 μM Tyr-L-MCa does not induce any specific cell death compared to the control condition (Fig. 1D, E). The control condition contained about 3.3% of dead cells compared to the 2.6% of the Tyr-L-MCa condition. In contrast, 5 min incubation with 0.1% saponin has a drastic effect on cell survival since the proportion of dead cells reached 93.4% (Fig. 1F). Similar results were obtained for a set of Tyr-L-MCa concentration that all indicate that this vector is non-toxic for F98 cells (Fig. 1G). Similar observations were made with F98 cells incubated with ^{125}I-Tyr-L-MCa indicating that gamma radiation did not

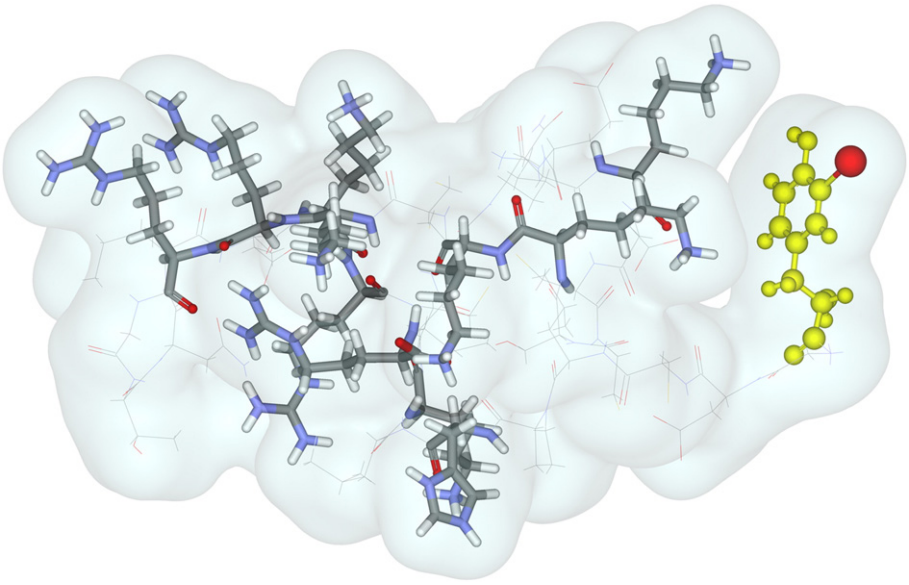

Fig. 2. Modeled 3D structure of ^{125}I-Tyr-L-MCa. The structure was modeled starting with L-MCa as a structural basis (1C6W from the Protein Database). The extra tyrosine residue is in yellow and the iodine on the tryrosine ring in red. The positively charged amino acid residues of L-MCa are also highlighted.

add a layer of cell toxicity in the frame of our experiments (data not shown).

3.3. Cell penetration properties of ^{125}I-Tyr-L-MCa

Production of the ^{125}I-Tyr-L-MCa compound with high radiochemical purity is an opportunity to quantify the cell penetration of L-MCa into cells. Earlier labeling of L-MCa with a fluorescence indicator provided only semi-quantitative information [11]. We first designed a subcellular fractionation protocol that was aimed at minimizing the contribution of any external membrane-attached ^{125}I-Tyr-L-MCa radioactivity associated to F98 cells. This protocol includes trypsin treatment, many cell washes, and a systematic transfer of the biological material to new plastic tubes in order to avoid possible attachment of any external ^{125}I-Tyr-L-MCa to plastic surfaces. Trypsin treatment was kept to the minimum because its first aim is to detach cells from the surface. Longer exposure would result in better external ^{125}I-Tyr-L-MCa degradation but also in cell damaging which is not desirable. Fig. 3 illustrates that indeed a 5 min trypsin digestion after F98 cell incubation with ^{125}I-Tyr-L-MCa results in only limited peptide degradation. The appearance on the HPLC elution profile of a new leftward-shifted peak, which is superimposed to the remnant

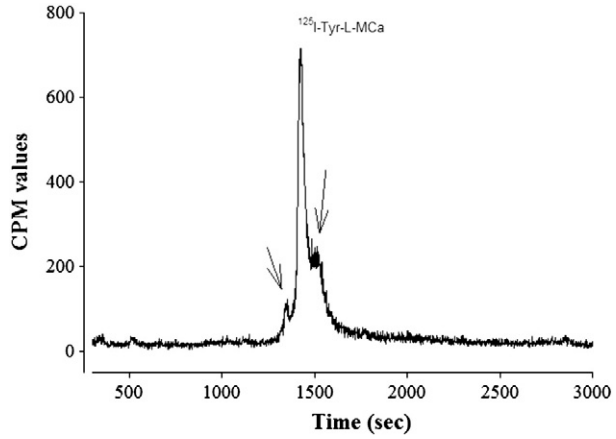

Fig. 3. RP-HPLC profile of ^{125}I-Tyr-L-MCa following 5 min of incubation with trypsin. The major peak is the intact ^{125}I-Tyr-L-MCa, while the peaks denoted by the arrows reflect degraded products.

peak of the original ^{125}I-Tyr-L-MCa compound, indicates that the trypsin-mediated degradation is only partial. To further minimize the potential quantitative contribution of any cell membrane-bound ^{125}I-Tyr-L-MCa, the plasma membrane was quantified as a separate entity and the radioactivity associated to this subcellular fraction was excluded from our calculations of L-MCa cell entry and accumulation. However, as we shall see later, the radioactivity associated with the plasma membrane was extremely low indicating little accumulation of the peptide in membrane fractions which further strengthens the reliance on the protocol used to quantify cell entry.

The entire study was performed on the rat glioblastoma cancer cell line F98 maintained in culture. To assess the cell concentration achieved by the ^{125}I-Tyr-L-MCa, we first determined two important parameters: i) the cell number in each well and ii) the average volume of F98 cells. The cell number in each culture well was established by FACS counting. The average cell number was 403,754 ± 23,434 per well (n = 4 wells). This includes 96.7% of live cells and 3.3% of dead cells as defined in Fig. 1D. Next, we evaluated the average cell volume using two different techniques: DHM and cell volume reconstruction through the acquisition of stacks of confocal images. Fig. 4A illustrates the optical thickness image produced by DHM with gray levels coding for the optical thickness. The surface reconstruction of the optical thicknesses is shown in Fig. 4B. The volume of F98 cells can be obtained by integration of the optical thickness inside the cell areas. A histogram illustrating individual cell volume was constructed (Fig. 4C). Fitting the data provides an average cell volume of $8.9 \times 10^{-7} \pm 0.2 \times 10^{-7}$ μl (n = 130 cells). We also used z-stacks of CM images to reconstruct cell volumes, again by focusing on individual cells. The boundaries of cells were provided by concanavalin-A rhodamine staining of the plasma membranes. Using this CM method instead of DHM, we come up with an average F98 cell volume of 18.9×10^{-7} μl (n = 95 cells). There is thus a 2.12-fold difference in volume estimation using these two methods. DHM is likely a more precise technique for volume estimation and we will rely on the average DHM value to calculate the intracellular concentration of ^{125}I-Tyr-L-MCa. However, when applicable, the concentration values will also be provided using the CM cell volume evaluation method in parentheses.

First, we investigated how dead cells may affect the uptake of ^{125}I-Tyr-L-MCa. The peptide being extremely basic it is possible that dead cells, by exposing their DNA or their protein content, may overly contribute to the measured signal. We therefore purposely compared

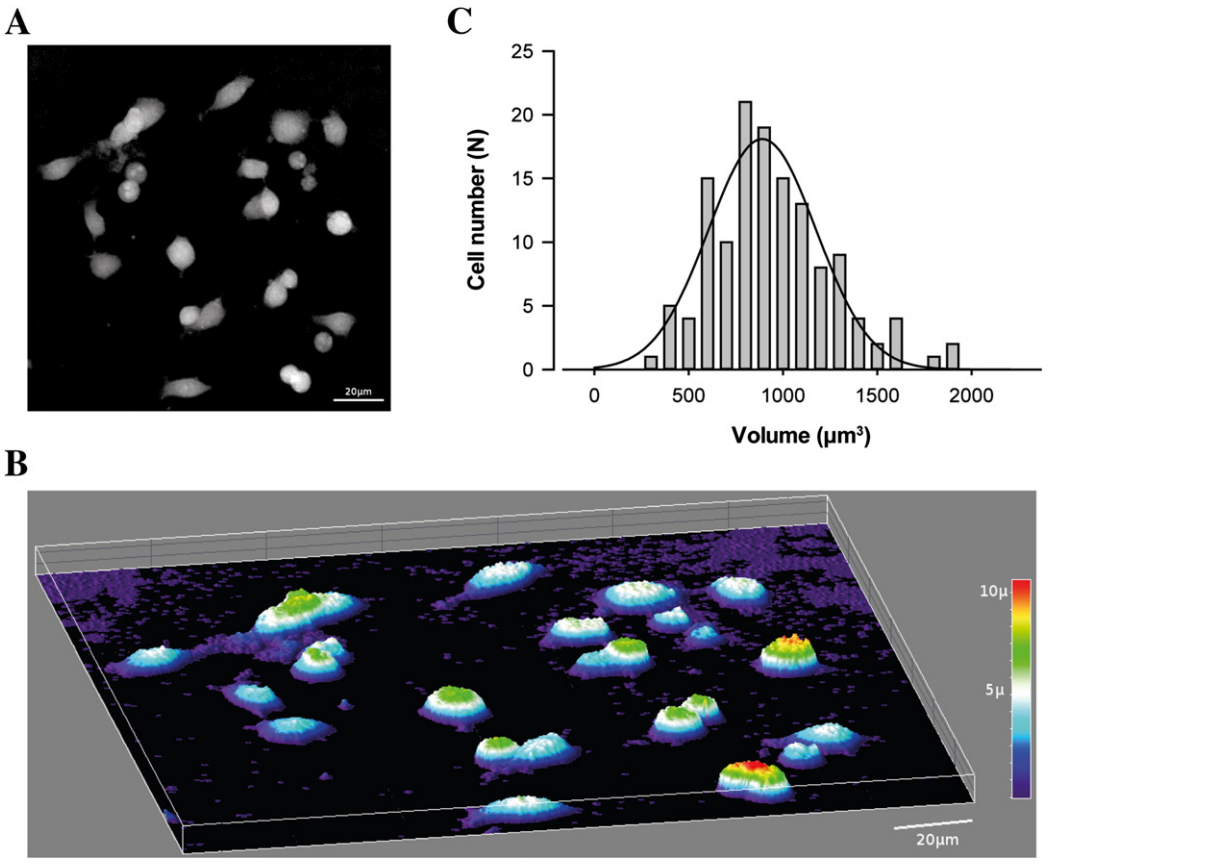

Fig. 4. Estimation of the average volume of F98 glioblastoma cells by DHM. (A) Optical thickness image produced by DHM, the gray levels are coding for the optical thickness. (B) Surface reconstruction of the optical thicknesses. (C) Histogram showing the distribution of individual cell volumes, obtained by integrating the optical thickness inside the cell areas. Only individual cells were used to evaluate cell volumes since touching cells could lead to overestimation. Cell fragments were also avoided for this analysis.

the amount of accumulated radioactivity in live cells incubated 2 h with 33 µM ^{125}I-Tyr-L-MCa with the amount found in dead cells, the cell death being promoted by 0.1% saponin. As shown in Fig. 5A, dead cells accumulate a surprisingly high level of radioactivity in each of the subcellular fractions. In each case however, the level of activity was lower than in live cells, indicating that cell death should not affect the measurements on live cells significantly. Fig. 5A also illustrates that the plasma membrane is the subcellular fraction that accumulates the least radioactivity compared to the cytoplasm and the nucleus. At this external concentration, the plasma membrane represents 9.4% of the accumulated radioactivity. In contrast, the cytoplasm and the nucleus of live cells accumulate each 25.6% and 64.7%, respectively. These proportions were however altered in dead cells with respective accumulations of 15.7% (plasma membrane), 45.1% (cytoplasm) and 32.2% (nucleus). The comparatively good accumulation of ^{125}I-Tyr-L-MCa in the cytoplasmic fraction of dead cells is probably linked to the effect of saponin on the plasma membrane. Since saponin should not affect the membrane of the nucleus, we still observe a quantitative difference in the accumulation of ^{125}I-Tyr-L-MCa radioactivity in dead cells compared to live ones. The result also indicates that the intracellular concentration of ^{125}I-Tyr-L-MCa should not exceed by far the extracellular concentration of the compound since passive accumulation within permeabilized cells resembles the accumulation within live cells.

We examined the concentration-dependent uptake of ^{125}I-Tyr-L-MCa by live F98 cells using extracellular concentrations ranging from 3.3 nM to 10 µM for a 2 hour-incubation time. We then assessed the cumulated radioactivity within each subcellular fraction. As shown in Fig. 5B, evident accumulation of ^{125}I-Tyr-L-MCa occurs essentially within the cytoplasm and the nucleus at a concentration as low as 300 nM. Increasing extracellular concentrations of the ^{125}I-Tyr-L-MCa also produce increasing elevations of the radioactivity within each fraction with similar dose-dependent profiles. In the result shown here, there was almost no accumulation within the plasma membrane fraction. There is no sign of saturation in full agreement with earlier observations using L-MCa tagged with fluorescent dyes [10,11]. The cell count, the average DHM-assessed F98 cell volume and the specific activity of ^{125}I-Tyr-L-MCa have been used to convert the experimental cpm data into average cell concentrations of ^{125}I-Tyr-L-MCa. Only cumulated cpm values from the cytoplasm and the nucleus were taken into account since the radioactivity associated to the plasma membrane fraction could bear some ^{125}I-Tyr-L-MCa from the outer leaflet of the membrane that would not be digested by the trypsin treatment as shown earlier. Obviously, this may lead to underestimation of the total accumulated ^{125}I-Tyr-L-MCa in F98 cells but this was preferable to a slightly overestimated concentration, the plasma membrane accounting for only a small fraction of the total radioactivity (<10% at all concentrations tested and for each experiment we performed). According to the method, we show a close correspondence in the intracellular concentration of ^{125}I-Tyr-L-MCa compared to the extracellular concentration (Fig. 5C). For instance at 1 µM external ^{125}I-Tyr-L-MCa, F98 cells accumulated 2.41 µM of the peptide according to DHM volume estimation (1.14 µM according to CM-based volume estimation). Examining the internal concentration of ^{125}I-Tyr-L-MCa as a function of the external concentration indicates that the concentration ratio (internal/external) is higher at lower external concentrations than at high external concentrations. This was marked at 10 nM where penetration is barely detected with this cell penetrating peptide. Fitting the experimental data with a decreasing exponential curve yields a concentration ratio of 2.45 according to DHM data (or 1.15 according to CM data) (Fig. 5C, inset).

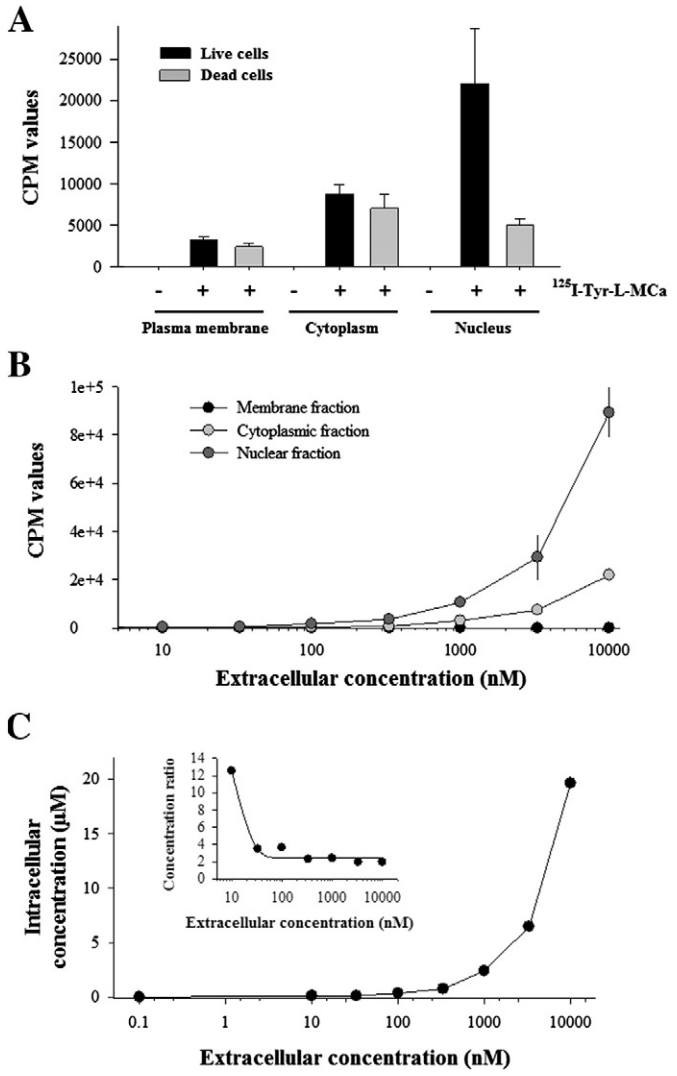

Fig. 5. Estimation of the accumulation properties of ^{125}I-Tyr-L-MCa in F98 cells. (A) Total radioactivity accumulated in subcellular fractions of live and dead cells (plasma membrane, cytoplasm, and nucleus). Radioactivity was also measured for control live cells in the absence of ^{125}I-Tyr-L-MCa. No significant counts could be measured. Extracellular concentration of ^{125}I-Tyr-L-MCa used: 33 µM. 2 h incubation. (B) Concentration dependent accumulation of ^{125}I-Tyr-L-MCa in subcellular fractions of live cells. 2 h of incubation with the radiochemical compound. (C) Evaluation of the internal concentration of ^{125}I-Tyr-L-MCa reached after 2 h incubation of live F98 cells as a function of the external concentration of ^{125}I-Tyr-L-MCa. Inset: ratio of concentration as a function of the external ^{125}I-Tyr-L-MCa. The data were fitted with the following equation $y = y_0 + a.e^{-bx}$ where $y_0 = 2.45 \pm 0.31$, $a = 27.1 \pm 8.6$ and $b = 0.098 \pm 0.031$.

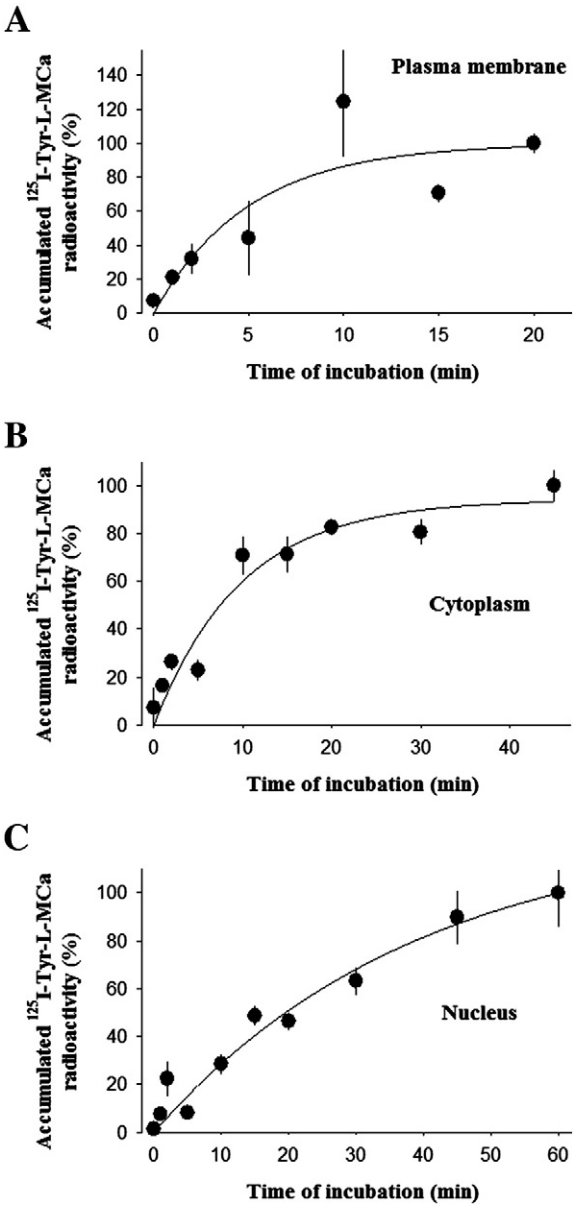

Fig. 6. Kinetics of ^{125}I-Tyr-L-MCa accumulation within the different subcellular compartments of F98 cells. (A) Kinetics of ^{125}I-Tyr-L-MCa accumulation within the plasma membrane fraction of F98 cells. The data were fitted with the equation $y = a \times (1 - e^{-bx})$ where $a = 99.8 \pm 19.7$ and $b = 0.20 \pm 0.12$ min^{-1}. (B) Kinetics of ^{125}I-Tyr-L-MCa accumulation within the cytoplasmic fraction of F98 cells. Parameters after fitting were: $a = 94.2 \pm 8.1$ and $b = 0.10 \pm 0.02$ min^{-1}. (C) Kinetics of ^{125}I-Tyr-L-MCa accumulation within the nuclear fraction of F98 cells. Parameters after fitting were: $a = 127.6 \pm 23.5$ and $b = 0.025 \pm 0.007$ min^{-1}. For all these experiments we used 1 µM of ^{125}I-Tyr-L-MCa.

3.4. Kinetics of entry and exit of ^{125}I-Tyr-L-MCa into and from F98 cells

For a ^{125}I-Tyr-L-MCa accumulation in the nucleus, the peptide needs first to cross the plasma membrane, then to accumulate within the cytoplasm, and should afterwards travel to the nucleus of F98 cells. This sequence of events requires that the kinetics of accumulation within each subcellular fraction should follow a logic time gradient. This point was investigated by incubating F98 cells with 1 µM ^{125}I-Tyr-L-MCa for various durations, fractionating the cells and counting the radioactivity associated to each fraction (Fig. 6). As shown, the time constant for radioactivity accumulation in the plasma membrane is $\tau = 5$ min (Fig. 6A). This value rises to $\tau = 10$ min for the cytoplasm (Fig. 6B), which remains quite rapid, and to $\tau = 20$ min for the accumulation in the nuclear fraction of F98 cells (Fig. 6C).

^{125}I-Tyr-L-MCa is heavily charged (net positive charge = +8) indicating that it may be attracted to the internal face of the plasma membrane because of the existence of the negative membrane potential. It can be envisioned that while the cell entry of the peptide is facilitated because of this membrane potential, the same negative charges residing in the cell may prevent the cell escape of the peptide. We investigated this issue by examining the gradual release of radioactivity within the external medium. As shown, F98 cells are extremely reluctant to release the radioactivity once accumulation has occurred (Fig. 7). It is only after 24 h of washout time that about 8.9% of the radioactivity is released by the cells.

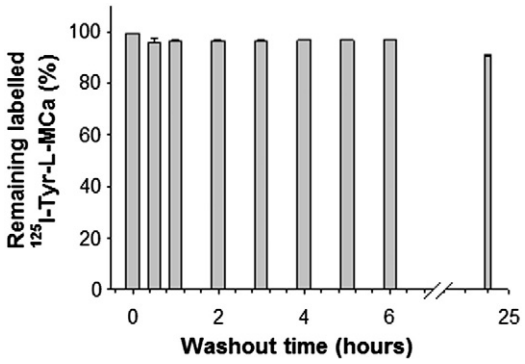

Fig. 7. Kinetics of cell exit rate of ^{125}I-Tyr-L-MCa from F98 cells. Time-dependent exit of ^{125}I-Tyr-L-MCa from F98 cells expressed as a percentage of total intracellular labeled peptide.

4. Discussion

L-MCa is the first example of a folded and oxidized animal peptide toxin acting as a CPP [6,8–12,14,21–24]. Since CPPs hold great promises in the field of drug delivery, it was therefore of great importance to determine the precise cell entry characteristics of L-MCa. Radiolabeling represents the most sensitive and quantitative method to quantify the cell entry of a molecule of interest. To this aim we produced Tyr-L-MCa that, as expected from earlier evidence, preserved proper folding and oxidation, as well as the original pharmacological properties of L-MCa and the resistance to proteolytic cleavage. The position of the extra tyrosine residue ensured that iodination occurred in a convenient way, without accessibility problems and without introducing structural disturbances within the native sequence. Compared to other reporting methods, the addition of an iodinated Tyr residue at the N-terminus of L-MCa keeps structural alterations of the peptide to a minimum.

For the first time, compared to all our earlier investigations using fluorochromes as reporters [10,11,14,21], we were able to extract valuable quantitative information on the cell penetration properties of ^{125}I-Tyr-L-MCa. For that purpose, we used the rat glioblastoma F98 cell line and several critical parameters to assess the penetration properties. First, we precisely defined the specific activity of ^{125}I-Tyr-L-MCa that allowed us to establish a precise correlation between measured cpm values and peptide quantities. Then, we used DHM to evaluate the cell volume and transform peptide quantities into intracellular concentrations. Finally, an adequate biochemical protocol combined to cell sub-fractionation helped defined cell compartments and informed on the relative cell distribution of ^{125}I-Tyr-L-MCa. It was striking to observe that very little radioactivity is associated to the plasma membrane fraction. This is coherent with earlier observations using MCa analogs coupled to fluorescent dyes. These vector/cargo couples were in most cases not observed at the plasma membrane level on images gathered by confocal microscopy, except on some occasions [10]. It was however possible that the lipophilic environment of the membrane could quench the fluorescence of these dyes. Our data using iodinated Tyr-L-MCa demonstrates that the plasma membrane is not a compartment of peptide accumulation on or in the cells. This indicates that the residency time of ^{125}I-Tyr-L-MCa within the plasma membrane is very low, a finding that is consistent with the fast kinetics of cell accumulation within the membrane. While the plasma membrane is an obligatory route of cell entry for ^{125}I-Tyr-L-M, the peptide must use unstable modes of interaction with the plasma membrane components. The transient nature of these interactions argues for a rapid crossing followed by a dilution process within the cytoplasm. The kinetics of accumulation within the cytoplasm is itself quite rapid (time constant of 10 min) but the degree of accumulation is significantly greater than in the plasma membrane. An interesting observation is the accumulation of the peptide within the nucleus, to a great proportion, indicating that the peptide that is transferred from the cytoplasm to the nucleus had to be freely moving in the cytoplasm and could not be trapped within endosomes. This wouldn't have occurred if the majority of the peptide had been captured in F98 cells by a form of endocytosis such as macropinocytosis. We were not able to assess the relative volumes occupied by the cytoplasm and the nucleus. These values would however be meaningless to some extent as both compartments are themselves sub-compartmentalized. However, the values of cpm accumulation within these two compartments were closely related suggesting that most likely passive equilibrium was reached in the concentrations of the labeled peptide. In any case, the finding that the peptide is present in the nucleus contradicts other observations using dyes or proteins as cargoes, as in all cases MCa analogs were mostly confined to the cytoplasmic region presumably because of cargo-oriented trapping into endosomes [8–12,14]. In other cases, however, we found evidence for nuclear accumulation of doxorubicin as cargo [22,25–27], indicating that the matter of nuclear accumulation is cargo dependent. The reason for the accumulation of ^{125}I-Tyr-L-MCa in the nucleus has not been investigated. However, it may be argued that the peptide freely crosses nuclear pores and passively invades the nucleus. Because of its basic nature, it may then be stabilized there by ionic interactions with DNA. This matter may be studied later by using some of the small cell penetrating peptide variants derived from L-MCa that lack the basic nature of the full-length peptide [10,14].

The kinetics of accumulation within the plasma membrane and the cytoplasm deserve another comment. The time constant of a few minutes for the cell penetration of ^{125}I-Tyr-L-MCa is in apparent contrast with the second time scale required for L-MCa to trigger Ca^{2+} release after external application [6]. This difference is unlikely to be due to the extra-tyrosine residue or its labeling with iodine. The ryanodine receptor activation requires less than 10 nM internal concentration. However because of the peculiar location of the binding site of L-MCa on the ryanodine receptor [5], at the interface of the cytoplasm and the plasma membrane, it is possible that local L-MCa elevations may suffice to activate the ryanodine receptor. This would further be exaggerated by the presence of up to four binding sites of L-MCa on the ryanodine receptor, with a single occupancy being sufficient for activation. In addition, significant Ca^{2+} signals are expected with the activation of very few ryanodine receptors. Finally, considering the lipophilic environment of the L-MCa binding site, the reversibility of interaction between L-MCa and the ryanodine receptor is not evident. For all these reasons, we therefore believe that the kinetics of cell entry and Ca^{m} release activation cannot be easily compared.

Regarding peptide concentrations reached within the cell, we found values indicating near passive distribution between the outside and the inside of the cell. Precise estimation of cell concentration of ^{125}I-Tyr-L-MCa is also linked to the precise estimation of cell volume. We purposely used two techniques of cell volume investigation and found closely related values. The close to 2-fold difference suggests that our concentration values can be corrected by a factor of 2 as well. In the worst-case scenario, the global concentration of the peptide inside cells would match the outside concentration of ^{125}I-Tyr-L-MCa. The estimated cell volume is of course the total cell volume and does not take into account the volume loss that should be introduced by the volume of many organelles such as mitochondria, endoplasmic reticulum and the Golgi apparatus for instance, if the peptide does not accumulate into these organelles. If we take this assumption as correct, then we may assume that part of the peptide accumulation may occur against the concentration gradient. Voltage-driven accumulation may well represent one mechanism explaining how cells may cumulate higher peptide concentrations than the outside. Cells are negatively polarized. The net positively charged L-MCa should be attracted by the negative charges located underneath the plasma membrane. A second potential mechanism may be local increases of the peptide concentration at the external side of the plasma membrane. L-MCa interacts with negatively charged glycosaminoglycans [24] or negatively charged lipids [8] and the positive charges of L-MCa may contribute to greater

interactions, thereby locally increasing the peptide concentration. In any case, the finding that the labeled peptide can barely escape the intracellular environment is also evidence for the existence of an accumulation process that is not only linked to passive redistribution of the peptide into the cells. It indicates the existence of a strong asymmetry in the fluxes of Tyr-L-MCa through the membrane. This may be linked to the asymmetric lipid composition or the existence again of a voltage gradient across the plasma membrane.

Acknowledgements

We thank the following platforms (GAIA, Prométhée, and microscopie optique from Université Joseph Fourier) for their collaboration. C. Tisseyre has a fellowship from Région Rhône-Alpes (cluster 11 Handicap, Vieillissement et Neurosciences). MDW thanks the French Agence Nationale de la Recherche (program Nanofret2 and LabEx "Ion Channel Science and Therapeutics", program number: ANR-11-LABX-0015) for financial support.

References

[1] M. Mae, U. Langel, Cell-penetrating peptides as vectors for peptide, protein and oligonucleotide delivery, Curr. Opin. Pharmacol. 6 (2006) 509–514.
[2] M. Pooga, U. Soomets, M. Hallbrink, A. Valkna, K. Saar, K. Rezaei, U. Kahl, J.X. Hao, X.J. Xu, Z. Wiesenfeld-Hallin, T. Hokfelt, T. Bartfai, U. Langel, Cell penetrating PNA constructs regulate galanin receptor levels and modify pain transmission *in vivo*, Nat. Biotechnol. 16 (1998) 857–861.
[3] M. Rhee, P. Davis, Mechanism of uptake of C105Y, a novel cell-penetrating peptide, J. Biol. Chem. 281 (2006) 1233–1240.
[4] A. Mosbah, R. Kharrat, Z. Fajloun, J.G. Renisio, E. Blanc, J.M. Sabatier, M. El Ayeb, H. Darbon, A new fold in the scorpion toxin family, associated with an activity on a ryanodine-sensitive calcium channel, Proteins 40 (2000) 436–442.
[5] X. Altafaj, W. Cheng, E. Esteve, J. Urbani, D. Grunwald, J.M. Sabatier, R. Coronado, M. De Waard, M. Ronjat, Maurocalcine and domain A of the II–III loop of the dihydropyridine receptor Cav 1.1 subunit share common binding sites on the skeletal ryanodine receptor, J. Biol. Chem. 280 (2005) 4013–4016.
[6] E. Esteve, K. Mabrouk, A. Dupuis, S. Smida-Rezgui, X. Altafaj, D. Grunwald, J.C. Platel, N. Andreotti, I. Marty, J.M. Sabatier, M. Ronjat, M. De Waard, Transduction of the scorpion toxin maurocalcine into cells. Evidence that the toxin crosses the plasma membrane, J. Biol. Chem. 280 (2005) 12833–12839.
[7] S. Mouhat, B. Jouirou, A. Mosbah, M. De Waard, J.M. Sabatier, Diversity of folds in animal toxins acting on ion channels, Biochem. J. 378 (2004) 717–726.
[8] S. Boisseau, K. Mabrouk, N. Ram, N. Garmy, V. Collin, A. Tadmouri, M. Mikati, J.M. Sabatier, M. Ronjat, J. Fantini, M. De Waard, Cell penetration properties of maurocalcine, a natural venom peptide active on the intracellular ryanodine receptor, Biochim. Biophys. Acta 1758 (2006) 308–319.
[9] K. Mabrouk, N. Ram, S. Boisseau, F. Strappazzon, A. Rehaim, R. Sadoul, H. Darbon, M. Ronjat, M. De Waard, Critical amino acid residues of maurocalcine involved in pharmacology, lipid interaction and cell penetration, Biochim. Biophys. Acta 1768 (2007) 2528–2540.
[10] C. Poillot, H. Bichraoui, C. Tisseyre, E. Bahemberae, N. Andreotti, J.M. Sabatier, M. Ronjat, M. De Waard, Small efficient cell-penetrating peptides derived from scorpion toxin maurocalcine, J. Biol. Chem. 287 (2012) 17331–17342.
[11] C. Poillot, K. Dridi, H. Bichraoui, J. Pecher, S. Alphonse, B. Douzi, M. Ronjat, H. Darbon, M. De Waard, D-Maurocalcine, a pharmacologically inert efficient cell-penetrating peptide analogue, J. Biol. Chem. 285 (2010) 34168–34180.
[12] T.-N.I., N. Ram, K. Pernet-Gallay, C. Poillot, M. Ronjat, A. Andrieux, C. Arnoult, J. Daou, M. De Waard, *In vitro* and *in vivo* cell delivery of quantum dots by the cell penetrating peptide maurocalcine, Int. J. Biomed. Nanosci. Nanotechnol. 2 (2011) 12–32.
[13] G.J. Stasiuk, S. Tamang, D. Imbert, C. Poillot, M. Giardiello, C. Tisseyre, E.L. Barbider, P.H. Fries, M. de Waard, P. Reiss, M. Mazzanti, Cell-permeable Ln(III) chelate-functionalized InP quantum dots as multimodal imaging agents, ACS Nano 5 (2011) 8193–8201.
[14] C. Tisseyre, E. Bahembera, L. Dardevet, J.M. Sabatier, M. Ronjat, M. De Waard, Cell penetration properties of a highly efficient mini maurocalcine Peptide, Pharm. (Basel) 6 (2013) 320–339.
[15] S. Mitra, T.S. Banerjee, S.K. Hota, D. Bhattacharya, S. Das, P. Chattopadhyay, Synthesis and biological evaluation of dibenz[b, f][1,5]oxazocine derivatives for agonist activity at kappa-opioid receptor, Eur. J. Med. Chem. 46 (2011) 1713–1720.
[16] E. Frampas, C. Maurel, P. Thedrez, P. Remaud-Le Saec, A. Faivre-Chauvet, J. Barbet, The intraportal injection model for liver metastasis: advantages of associated bioluminescence to assess tumor growth and influences on tumor uptake of radiolabeled anti-carcinoembryonic antigen antibody, Nucl. Med. Commun. 32 (2011) 147–154.
[17] Z. Fajloun, R. Kharrat, L. Chen, C. Lecomte, E. Di Luccio, D. Bichet, M. El Ayeb, H. Rochat, P.D. Allen, I.N. Pessah, M. De Waard, J.M. Sabatier, Chemical synthesis and characterization of maurocalcine, a scorpion toxin that activates Ca(2+) release channel/ryanodine receptors, FEBS Lett. 469 (2000) 179–185.
[18] R.B. Merrifield, Solid-phase peptide synthesis, Adv. Enzymol. Relat. Areas Mol. Biol. 32 (1969) 221–296.
[19] E. Cuche, F. Bevilacqua, C. Depeursinge, Digital holography for quantitative phase-contrast imaging, Opt. Lett. 24 (1999) 291–293.
[20] B. Rappaz, P. Marquet, E. Cuche, Y. Emery, C. Depeursinge, P. Magistretti, Measurement of the integral refractive index and dynamic cell morphometry of living cells with digital holographic microscopy, Opt. Express 13 (2005) 9361–9373.
[21] N. Ram, N. Weiss, I. Texier-Nogues, S. Aroui, N. Andreotti, F. Pirollet, M. Ronjat, J.M. Sabatier, H. Darbon, V. Jacquemond, M. De Waard, Design of a disulfide-less, pharmacologically-inert and chemically-competent analog of maurocalcine for the efficient transport of impermeant compounds into cells, J. Biol. Chem. 283 (2008) 27048–27056.
[22] S. Aroui, N. Ram, F. Appaix, M. Ronjat, A. Kenani, F. Pirollet, M. De Waard, Maurocalcine as a non toxic drug carrier overcomes doxorubicin resistance in the cancer cell line MDA-MB 231, Pharm. Res. 26 (2009) 836–845.
[23] A. Jayagopal, Y.R. Su, J.L. Blakemore, M.F. Linton, S. Fazio, F.R. Haselton, Quantum dot mediated imaging of atherosclerosis, Nanotechnology 20 (2009) 165102.
[24] N. Ram, S. Aroui, E. Jaumain, H. Bichraoui, K. Mabrouk, M. Ronjat, H. Lortat-Jacob, M. De Waard, Direct peptide interaction with surface glycosaminoglycans contributes to the cell penetration of maurocalcine, J. Biol. Chem. 283 (2008) 24274–24284.
[25] S. Aroui, S. Brahim, M. De Waard, J. Breard, A. Kenani, Efficient induction of apoptosis by doxorubicin coupled to cell-penetrating peptides compared to unconjugated doxorubicin in the human breast cancer cell line MDA-MB 231, Cancer Lett. 285 (2009) 28–38.
[26] S. Aroui, S. Brahim, M. De Waard, A. Kenani, Cytotoxicity, intracellular distribution and uptake of doxorubicin and doxorubicin coupled to cell-penetrating peptides in different cell lines: a comparative study, Biochem. Biophys. Res. Commun. 391 (2010) 419–425.
[27] S. Aroui, S. Brahim, J. Hamelin, M. De Waard, J. Breard, A. Kenani, Conjugation of doxorubicin to cell penetrating peptides sensitizes human breast MDA-MB 231 cancer cells to endogenous TRAIL-induced apoptosis, Apoptosis 14 (2009) 1352–1365.